

Novel lysophosphatidic acid receptor 6 antagonists inhibit hepatocellular carcinoma growth through affecting mitochondrial function

Davide Gnocchi ¹; Saketh Kapoor ²; Patrizia Nitti ³; Maria Maddalena Cavalluzzi ⁴; Giovanni Lentini ⁴; Nunzio Denora ⁴; Carlo Sabbà ¹ & Antonio Mazzocca ^{1*}

¹ Interdisciplinary Department of Medicine, University of Bari School of Medicine, Piazza G. Cesare, 11 - 70124 Bari, Italy

² Stem Cells and Regenerative Medicine Centre, Yenepoya Research Centre, Yenepoya (Deemed to be University), University Road, Derlakatte, Mangalore, Karnataka, 575018, India

³ Department of Chemical Sciences, University of Trieste, via Licio Giorgieri 1, I-34127 Trieste, Italy

⁴ Department of Pharmacy - Drug Sciences, University of Bari Aldo Moro, via Orabona, 4 - 70125 Bari, Italy

***Corresponding author:** Antonio Mazzocca, MD, PhD, Interdisciplinary Department of Medicine, University of Bari School of Medicine, Piazza G. Cesare, 11 - 70124 - Bari, Italy.
Tel.: +39-080-5593-593, **Fax:** +39-080-5593-593, **E-mail:** antonio.mazzocca@uniba.it

Financial Information: This work was supported by AIRC (Italian Association for Cancer Research) Investigator Grant (IG) 2015 Id.17758 (to A. Mazzocca).

Running Title: Anti-LPAR6 therapeutic approach for HCC (60 characters with spaces)

Keywords: hepatocellular carcinoma (HCC); lysophosphatidic acid receptor 6 (LPAR6); lysophosphatidic acid receptor 6 antagonists, drug discovery and design; drug therapy.

Conflict of Interest Statement: Authors have no potential conflicts of interest to disclose

Abstract

Hepatocellular carcinoma (HCC) is one of the most prevalent cancers worldwide and the most common liver cancer. It is expected to become the third leading cause of cancer-related deaths in Western Countries by 2030. This alarming trend can be explained with the increasing incidence of metabolic disorders (i.e. obesity, metabolic syndrome and diabetes), in addition to the major known risk factors such as hepatitis C or B viruses, and alcohol consumption. Effective pharmacological approaches for HCC are still unavailable, and the currently approved systemic treatments are unsatisfactory in terms of therapeutic results showing many side effects. Thus, searching for new effective and nontoxic molecules for HCC treatment is of paramount importance. We previously demonstrated that lysophosphatidic acid (LPA) is a central trigger in the pathogenesis of HCC and that lysophosphatidic acid receptor 6 (LPAR6) actively supports HCC tumorigenicity. Here, we screened for novel LPAR6 antagonists and found that two compounds, 4-methylene-2-octyl-5-oxotetra-hydrofuran-3-carboxylic acid (C75) and 9-xantenylacetic acid (XAA), efficiently inhibit HCC growth, both in vitro and in vitro, without displaying toxic effects at the effective doses. We further investigated the mechanisms of action of C75 and XAA and found that these compounds determine a G1-phase cell cycle arrest, without inducing apoptosis at the effective doses. Moreover, we found that both compounds act on mitochondrial homeostasis, by increasing mitochondrial biogenesis and reducing mitochondrial membrane potential. Overall, our results show two newly identified LPAR6 antagonists with a concrete potential to be translated into effective and side-effect free molecules for HCC therapy.

Abbreviations: HCC: hepatocellular carcinoma; LPARs: lysophosphatidic acid receptors; ATX: autotaxin; CAF: carcinoma associated fibroblasts; SRB: sulforhodamine B; NAFLD: non-alcoholic fatty liver disease; NASH: non-alcoholic steatohepatitis; MetS: metabolic syndrome; COX1: cytochrome c oxidase; COX2: cytochrome c oxidase subunit 2; β 2-MG: β 2-Microglobulin.

Introduction

Hepatocellular carcinoma (HCC) represents the sixth cause of cancer-related deaths worldwide and it is estimated to become the third cause in Western countries by 2030, despite the reducing incidence of chronic hepatitis infections (1). This trend can be explained by considering the increasing incidence of metabolic diseases. In fact, Non-Alcoholic Fatty Liver Disease is nowadays considered one of the leading causes of HCC, and convincing evidence supports the association between metabolic syndrome (MetS), diabetes, obesity and HCC in NAFLD patients. Additionally, diabetes is an independent risk factor for HCC, along with tobacco use (2). Treatment of HCC is mainly based on surgical approaches, such as resection, transplantation, ablation and trans-arterial chemoembolization. Pharmacological approaches rely on tyrosine-kinase inhibitors, such as *sorafenib*, *regorafenib* and *levantinib* (2), alone or in combination with immunotherapy drugs such as pembrolizumab and nivolumab (3). Still, these kinds of approaches show many adverse effects that make them not well tolerated from patients in the long term (4,5). Hence, the need to find novel effective and well-tolerated therapeutics for treating HCC is of primary importance. Several signaling pathways are involved in HCC development and progression, and, among them the ATX-LPA axis was shown to be particularly important (6,7). We have previously shown that lysophosphatidic acid (LPA) is actively involved in the pathogenesis of HCC, mediating the trans-differentiation of peritumoral tissue fibroblasts (PTFs) in carcinoma associated fibroblasts (CAF) (8). We also found that LPA receptor 6 (LPAR6) is required for supporting the tumorigenicity of HCC (9). In addition, we demonstrated that overexpression of LPAR6 resulted in a worse clinical outcome in patients with HCC (9). Starting from this background, we aimed to extend this knowledge in the attempt to identify novel molecules capable of effectively inhibiting LPAR6-driven HCC growth with less side effects if compared to the currently available therapeutic approaches. The idea was to target LPAR6 with specific molecules that could antagonize its activity and hence prospectively work as therapeutics agents. This work was therefore directed at screening and investigating the effect and the efficacy of novel potential LPAR6 antagonists as antitumor agents in HCC. Our preliminary screening identified two promising candidates, namely 4-methylene-2-octyl-5-oxotetra-hydrofuran-3-carboxylic acid (C75) and 9-xantylacetic acid (XAA), which showed significant anti-

proliferative effects both in vitro and in vivo at therapeutic doses without any toxicity. We further characterized these compounds pharmacologically, investigating the mechanisms of action: from this analysis emerged that both C75 and XAA affect cell cycle progression by causing a G1-phase arrest. We also investigated if C75 and XAA could affect the apoptotic process and found that only C75 induced apoptosis at supratherapeutic concentrations, while XAA did not show any effect. We additionally demonstrated that both C75 and XAA affect the mitochondrial homeostasis by increasing the mitochondrial biogenesis and by decreasing the mitochondrial membrane potential. These findings, together with the observed increase in intracellular lactate production, provide a mechanism explaining the cytostatic effect exerted by C75 and XAA. Thus, our observations support the potential of these novel LPAR6 antagonists to be translated into new anticancer therapeutics for the treatment of HCC.

Material and Methods

Ethics statement

All animal procedures were conducted in accordance with the national and international Guidelines for the Care and Use of Laboratory and were approved by the local Institutional Animal Care and Use Committee.

Reagents and antibodies

Sorafenib was purchased from Cell Signaling Technology [cat. #8705]. HA130 was purchased from Cayman Chemicals [cat. #10498] and AM966 was purchased from Cayman Chemicals [cat. #22048].

C75, MS95, OPBA, Q290, VS4 and XAA, were synthesized in collaboration with a chemical synthesis laboratory. The chemical structure of these compounds was designed according to their affinity for the binding site of LPAR6. The synthesis procedure followed for C75 and XAA is reported below. The detailed synthesis method is described in the Supplementary Data and illustrated in Supplementary Figures S1 and S2.

C75: C75 [(+)-(2*R*,3*S*)-1] was obtained with high enantioselectivity (98% ee) by kinetic enzymatic resolution of the corresponding racemic methyl ester, as previously described (10). Detailed chemical synthesis reactions are depicted in Supplementary Figure S1.

XAA: 9-Xanthenylacetic acid (XAA) was synthesized by reacting 9-hydroxyxanthene with malonic acid in acetic acid to give 9-xanthenylmalonic acid, which was then submitted to decarboxylation in pyridine (75% overall yield). Detailed chemical synthesis reactions are depicted in Supplementary Figure S1.

Cell lines and cell culturing

HepG2, Huh7, HLE cell lines were purchased from JCRB Cell Bank. HLE cell line overexpressing LPAR6 was generated in our laboratory as previously described (9). Human HCC cell lines and carcinoma-associate fibroblasts (CAFs) were isolated and cultured as previously described (8,9). HLE-neo and HLE-LPAR6 were grown in RPMI [Corning cat. # 10-041-CVR] supplemented with 10% FBS [Corning cat. # 35-079-CV]. HepG2 and Huh7 were grown DMEM [Corning cat. # 10-014-CVR] supplemented with 10% FBS [Corning cat. # 35-079-CV].

All drugs used were diluted in DMSO [Corning cat. # 25-950-CQC] (Vehicle) and treatments were

performed using volumes not exceeding 1% volume of the cell culture media. DMSO was used as vehicle control at 0.5% or 1% volume of the cell culture media.

For cell cycle experiments, cells were serum starved for 24 hours when at 35% confluency and successively treated in full media for the indicated times.

Cell proliferation assays

End-point proliferation was assayed by Crystal Violet staining after 72 hours drug incubation. Crystal Violet [Sigma-Aldrich cat. #C3886] was diluted in EtOH/H₂O 10% v/v to obtain a 1 mg/mL solution. Cells were fixed in 4% paraformaldehyde before adding CV. The color was eluted with 10% acetic acid and absorbance was read using an iMark™ plate reader [Bio-Rad cat. #168-1135] at $\lambda=595$ nm.

Toxicity assays

For Neutral Red assay [Invitrogen cat. #N3246] determination, the powder was diluted in DPBS to get a 0.33% solution, which was filtered in order to remove particulate. This solution was added in the culture media (10% v/v), and after 3 hours incubation at 37°C media was removed. After PBS washing the color was eluted using a 1% acetic acid solution in 50% ethanol. Absorbance was read using an iMark™ plate reader at $\lambda=540$ nm.

For MTT assay [SIGMA cat. #M2128], the powder was diluted in DPBS to obtain a 5 mg/mL solution. This solution was added in the culture media (10% v/v), and after 4 hours incubation at 37°C media was removed. The color was eluted using an acidified isopropanol solution with 1% Triton X-100 prepared as follows: 0.1 M HCl in isopropanol 100%+ Triton X-100 [Sigma-Aldrich cat. #T9284]. Absorbance was read using an iMark™ plate reader at $\lambda=570$ nm.

For protein determination, Bradford solution [Bio-Rad cat. #500-0006] was diluted before the assay as suggested by the producer. A standard curve was built using a BSA standard [Pierce cat. #23209]. Protein concentration was determined after reading absorbance with an iMark™ plate reader at $\lambda=595$ nm.

Migration assay

Migration and invasion assays were carried out using Boyden Chambers and Whatman filters [cat.

#150446] as previously described (8,9). Briefly, 1.5×10^5 - 2×10^5 cells suspended in 500 μL of serum-free media supplemented with 0.2% BSA were loaded in the upper part of a Boyden chamber, whose bottom part was filled with 200 μL of complete growth media with 10% FBS. Cells were let to migrate overnight, and filters were then methanol-fixed and stained with Crystal Violet. Cell counting was performed at the optical microscope.

G-protein-coupled receptor activation

Activation of LPAR6 and PAF receptor were evaluated by a TGF- α shedding assay as described by Inoue et al. (11). Briefly, the principle of the assay is the measurement of LPAR6 G protein-coupled receptor (GPCR) activity by a transforming growth factor- α (TGF α) shedding assay in which GPCR activation is quantified by the release in the conditioned medium of the ectodomain of a membrane-bound pro-form of alkaline phosphatase-tagged TGF- α (pro-AP-TGF- α), which work as a reporter gene.

Inhibition of ATX activity

The inhibition of ATX activity was evaluated by means of a colorimetric assay kit [Cayman chemicals, cat. #700580], based on the ATX cleaving activity on bis-(p-nitrophenyl) phosphate, which leads to the liberation of p-nitrophenol, a yellow product, whose absorbance is read at 415 nm.

3D Collagen co-culture assay

For three-dimensional (3D) co-culture experiments, Huh7-GFP and CAFs were seeded in a 1:1 ratio in a mixture of type I collagen neutralized with sodium hydroxide as previously described (8). Briefly, cultures were maintained for 96 hours, and the medium was changed every 48 hours. Cells were removed on the harvesting day and the GFP-positive cells used were counted by immunofluorescence microscopy. C75 and XAA were added to the cultures at a final concentration of 10 μM .

L-Lactate assay

Intracellular L-Lactate production was evaluated using a colorimetric kit [ScienCell cat. #8308]

according to the procedure suggested by the manufacturer. Briefly, a tetrazolium salt is reduced in a NADH-coupled enzymatic reaction to produce a colored formazan product. Absorbance was read using an iMark™ plate reader at $\lambda=490$ nm.

Cell cycle analysis by propidium iodide staining

Cell cycle analysis was performed using a Guava EasyCyte benchtop flow cytometer [Merck cat. #0500-5009] employing the Guava Cell Cycle Assay [Merck cat. #4500-0220] following producers' instructions. Briefly, culture media was collected and cells were washed twice with PBS, collecting PBS after the wash to obtain the whole cell population, including detached cells. Cells were then detached from culturing support by using trypsin and added to the collected media and PBS. After centrifugation, cells were resuspended in PBS+2%FBS to wash culturing media, centrifuged again and resuspended in 200 μ L PBS+2%FBS. Cells were eventually added dropwise to ice-cold 70% ethanol for fixation and permeabilization. After at least 24 hours fixation at 4° C, ethanol was removed by centrifugation, and after a PBS wash, the reagent was added. Acquisition was performed after a 30 minutes incubation in the dark.

Apoptosis evaluation

Induction of apoptosis by C75 and XAA was evaluated using a Guava EasyCyte benchtop flow cytometer [Merck cat. #0500-5009] employing the "Nexin" kit [Merck cat. #4500-0450] following producers' instructions. The kit detects the externalization of phosphatidylserine using Annexin V, in addition to the detection of late apoptotic/necrotic cells by the fluorescent exclusion dye 7-AAD. Briefly, culture media was collected and cells were washed twice with PBS collecting PBS after the wash in order to obtain the whole cell population, including detached cells. Then, trypsinized cells were detached from culturing support and added to the collected media and PBS. After centrifugation, cells were resuspended in complete growth media in order to get a suspension with 1×10^6 cells/mL. 1×10^5 cells were then diluted 1:1 with the Nexin reagent.

Mitotracker staining

Mitotracker [Invitrogen cat. #M7513] staining was performed according to the protocol described by Chazotte (12). Briefly, cells were grown on glass coverslips until they reached about 85%

confluence. Cells were then treated for 24 hours with C75, XAA and vehicle. After staining, images were acquired using a fluorescence microscope.

JC-1 staining

JC-1 [Invitrogen cat. #T3168] staining was performed according to the protocol described by Chazotte (13). Briefly, cells were grown on glass coverslips until they reached about 85% confluence. Cells were then treated for 24 hours with C75, XAA and vehicle. After staining, images were acquired using a fluorescence microscope.

Real-time quantitative PCR (RT-QPCR)

Total RNA was extracted using the Bio-Rad “Aurum RNA Mini kit” [Bio-Rad cat. #732-6820], following producer’s instructions. RNA amount and quality were evaluated by Invitrogen Nanodrop spectrophotometer.

cDNA was retrotranscribed using the Bio-Rad “iscript cDNA synthesis advanced kit” [Bio-Rad cat. #1725038] following producer’s instructions.

RT-QPCR was performed using the Bio-Rad “SsoAdvanced Universal SYBR Green Supermix” [Bio-Rad cat. #172-5275]. Fluorescence was read with an Applied Biosystem 7300 machine.

Primers used are available upon request.

Immunoelectrophoretic analyses

Cell lysates were done using a lysis buffer purchased from Cell Signaling [Cell Signaling cat. #CS 9803], supplemented with protease and phosphatase inhibitors [Roche cat. #04 693 159 001], [Roche cat. #04 906 837 001]. Proteins were separated by SDS-PAGE and blotted on nitrocellulose using a Bio-Rad semidry apparatus [Bio-Rad cat. #170-3940].

Primary antibody incubation was performed overnight at 4°C with gentle shaking, while secondary antibody incubation for 1 h at room temperature with gentle shaking. Revelation of bands was done by ECL with the Bio-Rad “Clarity” reagent [Bio-Rad cat. #170-5060S], using a Licor c-Digit apparatus.

Animal experiments

For the evaluation of tumorigenicity after subcutaneous implantation, 4- to 5-week-old female CD-1 nude (nu/nu) athymic mice were subdivided into four groups. The mice were housed and received food and water ad libitum. Huh7 from mid-log phase cultures were counted and then resuspended in a 50% mixture of Matrigel (BD Biosciences) in PBS. A 0.2 mL volume of the cell suspension containing 5.0×10^6 cells/mouse was injected s.c. in the right flank of each mouse. C75, XAA and saline were injected intrasplenically according to the scheduled administration procedure (thrice/week for five weeks). For co-injection experiments, a 1:1 ratio of tumor cells and CAF (5.0×10^6 cells each cell type/mouse) was injected. Tumor dimensions and body weights were recorded twice weekly. Tumor sizes (mm^3) were calculated using the equation $(w^2 \times l)/2$, where “w” and “l” refer to the width (mm) and length (mm) recorded at each measurement. Neoplastic progression was monitored based on the general health of the animals.

Statistical analyses

Survival curves were analyzed by means of the Kaplan-Meier method and the log-rank test for evaluating the difference between curves. In all other experiments One-Way ANOVA followed by Dunnett’s post-hoc test determined statistical significance. Normality was preliminary checked with D’Agostino-Pearson’s Omnibus K2 test. Statistical analyses and graph were performed with Graphpad Prism6 software.

Results

Novel LPAR6 antagonists effectively inhibit HCC growth

We preliminarily tested the effect of a set of potential LPAR6 antagonists selected on the basis of the LPA chemical structure similarity (Table 1). The anti-proliferative activity of these compounds was assessed in HepG2 and Huh7, two endogenously LPAR6-expressing HCC cell lines (14), and in the HLE HCC cell line genetically modified in our laboratory to stably overexpress LPAR6 (HLE-LPAR6). The relative levels of expression of LPAR6 in these three cell lines are shown in Supplementary Fig. S3A. Amongst the screened compounds, C75 (4-methylene-2-octyl-5-oxotetrahydrofuran-3-carboxylic acid) and XAA (9-xantenylacetic acid), displayed a significant anti-proliferative effect, comparable to that of *sorafenib*, a clinically available multi-kinase inhibitor used for HCC treatment, and of HA130, a well-established LPA antagonist (Fig. 1A and B). This anti-proliferative effect was mirrored in 2D and 3D co-culturing experiments using HCC cell lines together with carcinoma associated fibroblasts (CAF) (Supplementary Fig. S4A and S4B). The selective activity of C75 and XAA on LPAR6 was assayed by TGF- α release in HLE-LPAR6 and in non-expressing LPAR6 parental cell line (HLE-neo). Upon C75 and XAA treatment, TGF- α release was inhibited in HLE-LPAR6 to the level of non-expressing LPAR6 cells (HLE-neo), thus indicating the selective effect of these compounds on LPAR6 (Fig. 1C). An ATX inhibitory effect of C75 and XAA was also observed as evaluated by an enzymatic assay (Fig. 1D). A growth kinetics analysis of C75 and XAA effect was further performed in HepG2, Huh7, and HLE-LPAR6, showing a significant reduction in the number of proliferating cells in the presence of C75 and XAA if compared to vehicle (Fig. 1E). Next, we evaluated the effect of C75 and XAA on LPA-induced migration in the same cell lines, finding that C75 and XAA significantly inhibited HCC cell motility (Fig. 1F). Importantly, a similar inhibitory effect of C75 and XAA was observed in CAF migration and in HCC-mediated CAF migration, as compared with conditioned medium (CM) from ATX^{-/-} cells (HepG2 ATX^{-/-} CM) and HA130 (Supplementary Fig. S4C and S4D).

To assess the in vivo effect of C75 and XAA, experiments were carried out in HCC-bearing mice. Mice were injected in the flank with Huh7 cells and at day 7 they were treated with C75 and XAA (10 mg/kg) thrice a week for five weeks. We found that C75 and XAA significantly inhibited HCC

growth (Fig. 2A), and that these compounds were selective on LPAR6, as demonstrated by decreased serum levels of TGF- α in treated mice compared with controls (Fig. 2B). Interestingly, the antitumor effect observed in C75 and XAA-treated mice was comparable with the impaired HCC growth observed in mice injected with LPAR6 (LPAR6-shRNA) or ATX knocked down cells (ATX-shRNA) (Fig. 2C). The levels of LPA and LPAR6 were significantly decreased in knocked down cells, as shown in Fig. 2D. The antitumor effect of C75 and XAA was also observed in mice co-injected with Huh7 and CAF, suggesting the capacity of these compounds to block the stromal-tumor interactions supporting HCC growth (Supplementary Fig. S4E and S4F).

Therapeutic doses of novel LPAR6 antagonists C75 and XAA arrest cell cycle progression and does not induce apoptosis in HCC

We first performed viability tests to obtain information about C75 and XAA toxicity. To ensure reliability of results, different assays, namely Trypan Blue dye exclusion test, MTT, Neutral Red, and Sulforhodamine B (SRB), were carried out. Protein content was measured with Bradford assay as an additional control. As shown in Fig. 3A-C, C75 and XAA did not exhibit toxic effects at the indicated doses when compared to vehicle in all different tests carried out. Importantly, C75 and XAA did not show any toxic side effects in mice as evaluated by change in body weight. In fact, no significant changes in the body weight of mice were observed after C75 and XAA treatment for five weeks/thrice a week (Fig. 3D and Fig.2A). No sign of toxicity including absence of gross pathological findings and histological features in the brain, liver, spleen and kidney were observed in the treated mice.

We next sought to evaluate the mechanism by which C75 and XAA inhibit tumor growth. We therefore analyzed cell cycle distribution in HLE-LPAR6 and Huh7 treated cells by flow cytometry after propidium iodide DNA staining. As a drug capable of arresting HCC cell cycle (15), *sorafenib* was used as positive control. The flow cytometric analysis revealed that C75 and XAA, similarly to sorafenib, induced a G1 phase arrest in both cell lines at the indicated doses (Fig. 4A). We next examined whether central cell cycle mediators, such as cyclin D1 (CYCD1) (16), cyclin D3 (CYCD3) (17), cell-division cycle protein 20 (CDC20) (18), cell-division cycle protein 25 (CDC25) (19) and the cyclin-dependent kinase inhibitor p21 (20), were involved in the cell cycle arrest of HCC cells upon treatment with C75 and XAA. To this end, we evaluated the

expression level of the above-mentioned genes after 24 hours treatment with C75 and XAA at 10 μ M concentration by using RT-qPCR. Our results show that these compounds significantly decreased the expression of *CYCD1*, *CYCD3*, *CDC20* and *CDC25* genes, and increased the expression of *P21*, a well-recognized promoter of cell cycle arrest, when compared to vehicle (Fig. 4B).

Then, we investigated the effect of C75 and XAA on apoptosis in HCC cells at the doses that we found to be effective in inhibiting cell growth. Apoptosis was evaluated analyzing phosphatidylserine externalization by annexin V staining by using the Guava bench cytofluorimeter “Nexin” reagent. Our results show that both C75 and XAA did not trigger apoptosis at the dose of 10 μ M in HLE-LPAR6 and Huh7 cells after 24 hours of incubation (Fig. 4C and D). To further support this observation, we evaluated the effect C75 and XAA on apoptosis at supratherapeutic doses of 80 μ M, using a high dose of sorafenib (20 μ M) as a positive control. Results reported in Supplementary Fig. S5 A-B clearly show that C75, at the dose of 80 μ M, determined a strong induction of apoptosis in both HLE-LPAR6 and Huh7 cells, even stronger if compared to that of 20 μ M sorafenib. Interestingly, XAA did not show any effect in triggering apoptosis even at these higher doses. To further support these observations on apoptosis, we performed a dose-response SRB viability assay, with concentrations of C75 and XAA ranging from 10 μ M to 80 μ M. Our results clearly indicate that C75 is toxic at high dose only (Supplementary Fig. S5), whereas XAA treatment did not result in any cell toxicity, even at 80 μ M (Supplementary Fig. S5 C). Finally, we verified if a long-term treatment (72 hours) with a 10 μ M dose could trigger apoptosis in HLE-LPAR6 cell line and found no apoptosis induction by C75 and XAA at the indicated doses (Supplementary Fig. S5 D).

Novel LPAR6 antagonists C75 and XAA affect mitochondrial function in HCC

To verify if C75 and XAA exert their cytostatic effect by acting on mitochondrial function, we analyzed the action of these compounds in mitochondrial homeostasis. In fact, it is known that mitochondrial functional parameters, such as biogenesis and mitochondrial membrane potential are functionally linked to cell proliferation and apoptosis. Particularly, it was shown that a decrease in mitochondrial membrane potential is associated with a G1 arrest in the cell cycle progression (21). A mitochondrial decreased copy number was also observed in many cancer

types, including HCC (22,23). In addition, a suppression in the mitochondrial respiratory gene expression was found in many cancers (24). We therefore tested if C75 and XAA could affect mitochondrial biogenesis and distribution. To assess these aspects, we used two different experimental approaches. Firstly, we decided to visualize mitochondrial number, size and distribution by staining mitochondria with Mitotracker, a specific fluorescent dye (12). Results reported in Fig. 5A show that in HLE-LPAR6, mitochondrial number was significantly increased upon a 24 hours treatment with C75 and XAA at the indicated doses as demonstrated by Mitotracker staining. Secondly, we monitored the expression levels of two marker genes for mitochondrial biogenesis, namely cytochrome c oxidase 1 (COX1) and cytochrome c oxidase 2 (COX2) by Real-Time Quantitative Reverse Transcription PCR (qRT-PCR). As shown in Fig. 5B, after a 24 hours treatment at the indicated doses, C75 and XAA determine a significant increase in COX1 and COX2 expression in HLE-LPAR6 cells if compared with vehicle. We also looked at the level of expression of the subunit 1 of NADH dehydrogenase (ND1) by qRT-PCR, expressed as ND1/ β 2-MG ratio. In line with COX1 and COX2 expression results, a 24-hour treatment with C75 and XAA at the indicated doses significantly increase ND1/ β 2-MG ratio in HLE-LPAR6 cells (Fig. 5C). Also, a significant reduction in mitochondrial membrane potential was observed in C75- and XAA-treated HLE-LPAR6 cells as shown in Fig. 5D. Finally, C75 and XAA significantly increased intracellular L-Lactate production in HLE-LPAR6 cells (Fig. 5E).

Discussion

Few drugs are currently clinically available for the treatment of HCC, which act as tyrosine kinase inhibitors, such as *sorafenib*, *regorafenib* or *levantinib*. Their efficacy is not satisfactory and they additionally display many toxic side effects. In this article, by screening several potential LPAR6 antagonists, we have shown that two compounds, *C75* and *XAA*, display a significant anti-proliferative effect in HCC both in vivo and in vitro, comparable to that of *sorafenib* in terms of effectiveness, but without the toxic effects exerted by *sorafenib*. *C75* was already known as a fatty acid synthase (FAS) inhibitor (25), and as an anti-tumor agent in some experimental models (26,27). In other experimental settings, the anti-proliferative and the pro-apoptotic effect of *C75* were observed at supratherapeutic doses (40-60 μM) and linked to the inhibition of FAS. Instead, we found a cytostatic effect with no cytotoxicity and without induction of apoptosis at the effective doses of 10 μM . This suggests that the effect of *C75* at the doses used in our study could be exerted mainly as a LPAR6 antagonist in HCC. In fact, the doses required for inhibiting LPAR6 are lower of those necessary to inhibit FAS activity. Conversely, *XAA* is a completely new compound that we synthesized in collaboration with a chemical synthesis laboratory. In most of the tests, the effect of *XAA* was very similar to that of *C75*, with the remarkable difference that *XAA* does not show any toxicity at higher doses. This aspect configures *XAA* as a very interesting compound, whose mechanisms of action and cellular targets will be more deeply investigated in future studies. Worth underlining here is that both *C75* and *XAA* are also effective in the inhibition of hepatocyte-fibroblast crosstalk, by exerting a direct effect towards cancer-associated fibroblasts (CAF). This aspect definitely strengthens the translational relevance of these compounds as novel anti-HCC drugs.

In conclusion, in this article, we demonstrated that two novel LPAR6 antagonists, *C75* and *XAA*, are very effective as anti-HCC compounds without significant toxicity, thus showing an excellent ratio between antitumor effect and cytotoxicity. This is a notable feature in the treatment of HCC, which generally arises in a compromised liver. Future investigation may further provide additional details and increase the knowledge about the mechanism of action of these compounds from a molecular point of view. In any case, from a translational perspective these molecules may prove excellent and very promising drugs in the therapy of HCC.

Figure Legends

Figure 1.

Novel LPAR6 antagonists C75 and XAA effectively inhibit HCC cell proliferation and migration. **A**, C75 and XAA effectively inhibit HCC proliferation. The anti-proliferative effect of novel LPAR6 antagonists was screened in three different in vitro HCC models (HepG2, Huh7, HLE-LPAR6). Cells were treated with the indicated compounds (10 μ M final concentration) or vehicle control (0.5% DMSO) for 72 hours. The number of proliferating cells was determined by crystal violet staining. Amongst the others, C75 and XAA showed a significant anti-proliferative effect, comparable with that of sorafenib; **B**, C75 and XAA chemical structure; **C**, C75 and XAA selectively target LPAR6 activity. HLE-neo and HLE-LPAR6 cells were treated with C75 and XAA (10 μ M final concentration) for 30 minutes. TGF α release was then determined as described in Materials and Methods section. **D**, C75 and XAA effectively decrease ATX activity. Cells were treated with C75 and XAA at the indicated doses for 30 minutes. ATX activity was then assessed by a colorimetric assay as described in Materials and Methods section. **E**, C75 and XAA significantly inhibit HCC proliferation. C75 and XAA effect was screened in three different in vitro HCC models (HepG2, Huh7, HLE-LPAR6). Cells were treated with C75 and XAA (10 μ M final concentration) or vehicle control (0.5% DMSO) for 96 hours. The number of proliferating cells was determined by Trypan Blue dye exclusion test. **F**, C75 and XAA significantly inhibit HCC migration. C75 and XAA effect was screened in three different in vitro HCC models (HepG2, Huh7, HLE-LPAR6 cell lines). Cells were treated with compounds (10 μ M final concentration) or vehicle control (0.5% DMSO) for 24 hours. * $p < 0.05$ as determined by one-way ANOVA analysis.

Figure 2.

Novel LPAR6 antagonists C75 and XAA effectively inhibit HCC growth in vivo. **A**, C75 and XAA (5 mg/kg) significantly reduce HCC growth. Mice were treated with compounds at the indicated dose at the indicated times. **B**, Effect of autotaxin (ATX) knockdown in Huh7 cells on tumor growth in mice. **C**, C75 and XAA (5 mg/kg) significantly reduce serum TGF α levels in

HCC xenograft mice. Mice were treated with compounds at the dose indicated above for 49 days. Serum TGF α concentration was determined by a colorimetric kit. **D**, LPA levels and LPAR6 expression in vivo after ATX knockdown. Serum LPA concentration was assessed by ELISA whereas LPAR6 gene expression was determined by RT-qPCR. The efficiency of ATX knockdown was verified by immunoblotting. * $p < 0.05$ as determined by one-way ANOVA analysis. ** $p < 0.01$ as determined by one-way ANOVA analysis.

Figure 3.

Novel LPAR6 antagonists C75 and XAA do not affect cell viability in liver cancer cell lines. **A**, Cell viability was assessed by Trypan Blue dye exclusion test. The indicated cell lines were treated with C75 and XAA at the indicated doses or vehicle control (0.5% DMSO) for 72 hours before cell counting; **B**, Cell viability was assessed by Neutral Red cytotoxicity test. The indicated cell lines were treated with C75 and XAA at the indicated doses or vehicle control (0.5% DMSO) for 72 hours before performing Neutral Red cytotoxicity test; **C**, The indicated cell lines were treated with C75 and XAA at the indicated doses or vehicle control (0.5% DMSO) for 72 hours before performing SRB cytotoxicity test; **D**, Toxicity in vivo was assessed by monitoring mice body weight up to 49 days after 35 days drug administration at a 5 mg/kg dose. *** $p < 0.001$ as determined by one-way ANOVA analysis. **** $p < 0.0001$ as determined by one-way ANOVA analysis.

Figure 4.

Novel LPAR6 antagonists C75 and XAA arrest HCC growth by targeting cell cycle without affecting apoptosis. **A**, Huh7 and HLE-LPAR6 cells were serum starved for 24 hours when at 30-35% confluency before treating with C75 and XAA for 24 hours at 10 μ M final concentration. Cell cycle distribution was determined by FACS analysis after propidium iodide staining using a Guava EasyCyte benchtop flow cytometer; **B**, Huh7 and HLE-LPAR6 cells were treated for 24 hours with C75 and XAA at the indicated doses, before RNA extraction. Gene expression was determined by RT-qPCR; **C**, HLE-LPAR6 and Huh7 cells were treated for 24 hours with C75 and XAA at the indicated doses before harvesting. Apoptosis was evaluated by Annexin V staining using a Guava EasyCyte benchtop flow cytometer. *** $p < 0.001$ as determined by one-way

ANOVA analysis. **** p<0.0001 as determined by one-way ANOVA analysis.

Figure 5.

Novel LPAR6 antagonists C75 and XAA affect mitochondrial biogenesis and membrane potential.

A, HLE-LPAR6 cells were treated for 24 hours with C75 and XAA at 10 μ M final concentration before staining with Mitotracker dye. Quantification of the staining was performed with FIJI-

ImageJ software; **B**, HLE-LPAR6 cells were treated for 24 hours with C75 and XAA at 10 μ M final concentration, before RNA extraction. COX-1 and COX-2 gene expression was determined

by RT-QPCR; **C**, HLE-LPAR6 cells were treated for 24 hours with C75 and XAA at 10 μ M final concentration before staining with JC-1 dye. Quantification of the staining was performed with

FIJI-ImageJ software; **D**, HLE-LPAR6 cells were treated for 24 hours with C75 and XAA at 10 μ M final concentration before intracellular L-Lactate production evaluation by a colorimetric

assay. * p<0.05 as determined by one-way ANOVA analysis. *** p<0.001 as determined by one-way ANOVA analysis. **** p<0.0001 as determined by one-way ANOVA analysis.

Acknowledgements

This work was supported by a research grant from AIRC (Italian Association for Cancer Research) to A. Mazzocca.

References

1. de Lope CR, Tremosini S, Forner A, Reig M, Bruix J. Management of HCC. *J Hepatol* **2012**;56 Suppl 1:S75-87 doi 10.1016/S0168-8278(12)60009-9.
2. Forner A, Reig M, Bruix J. Hepatocellular carcinoma. *Lancet* **2018**;391(10127):1301-14 doi 10.1016/S0140-6736(18)30010-2.
3. Kudo M. Systemic Therapy for Hepatocellular Carcinoma: Latest Advances. *Cancers (Basel)* **2018**;10(11) doi 10.3390/cancers10110412.
4. Waidmann O. Recent developments with immunotherapy for hepatocellular carcinoma. *Expert Opin Biol Ther* **2018**;18(8):905-10 doi 10.1080/14712598.2018.1499722.
5. Wu Z, Lai L, Li M, Zhang L, Zhang W. Acute liver failure caused by pembrolizumab in a patient with pulmonary metastatic liver cancer: A case report. *Medicine (Baltimore)* **2017**;96(51):e9431 doi 10.1097/MD.00000000000009431.
6. Kaffe E, Katsifa A, Xylourgidis N, Ninou I, Zannikou M, Harokopos V, *et al.* Hepatocyte autotaxin expression promotes liver fibrosis and cancer. *Hepatology* **2017**;65(4):1369-83 doi 10.1002/hep.28973.
7. Nakagawa S, Wei L, Song WM, Higashi T, Ghoshal S, Kim RS, *et al.* Molecular Liver Cancer Prevention in Cirrhosis by Organ Transcriptome Analysis and Lysophosphatidic Acid Pathway Inhibition. *Cancer Cell* **2016**;30(6):879-90 doi 10.1016/j.ccell.2016.11.004.
8. Mazzocca A, Dituri F, Lupo L, Quaranta M, Antonaci S, Giannelli G. Tumor-secreted lysophosphatidic acid accelerates hepatocellular carcinoma progression by promoting differentiation of peritumoral fibroblasts in myofibroblasts. *Hepatology* **2011**;54(3):920-30 doi 10.1002/hep.24485.
9. Mazzocca A, Dituri F, De Santis F, Filannino A, Lopane C, Betz RC, *et al.* Lysophosphatidic acid receptor LPAR6 supports the tumorigenicity of hepatocellular carcinoma. *Cancer Res* **2015**;75(3):532-43 doi 10.1158/0008-5472.CAN-14-1607.
10. Chakrabarty K, Defrenza I, Denora N, Drioli S, Forzato C, Franco M, *et al.* Enzymatic resolution of alpha-methyleneparaoic acids and evaluation of their biological activity. *Chirality* **2015**;27(3):239-46 doi 10.1002/chir.22419.
11. Inoue A, Ishiguro J, Kitamura H, Arima N, Okutani M, Shuto A, *et al.* TGFalpha shedding assay: an accurate and versatile method for detecting GPCR activation. *Nat Methods* **2012**;9(10):1021-9 doi 10.1038/nmeth.2172.
12. Chazotte B. Labeling mitochondria with MitoTracker dyes. *Cold Spring Harb Protoc* **2011**;2011(8):990-2 doi 10.1101/pdb.prot5648.
13. Chazotte B. Labeling mitochondria with JC-1. *Cold Spring Harb Protoc* **2011**;2011(9) doi 10.1101/pdb.prot065490.
14. Sokolov E, Eheim AL, Ahrens WA, Walling TL, Swet JH, McMillan MT, *et al.* Lysophosphatidic acid receptor expression and function in human hepatocellular carcinoma. *J Surg Res* **2013**;180(1):104-13 doi 10.1016/j.jss.2012.10.054.
15. Sonntag R, Gassler N, Bangen JM, Trautwein C, Liedtke C. Pro-apoptotic Sorafenib signaling in murine hepatocytes depends on malignancy and is associated with PUMA expression in vitro and in vivo. *Cell Death Dis* **2014**;5:e1030 doi 10.1038/cddis.2013.557.
16. Qie S, Diehl JA. Cyclin D1, cancer progression, and opportunities in cancer treatment. *J Mol Med (Berl)* **2016**;94(12):1313-26 doi 10.1007/s00109-016-1475-3.
17. Das SK, Hashimoto T, Kanazawa K. Growth inhibition of human hepatic carcinoma HepG2

cells by fucoxanthin is associated with down-regulation of cyclin D. *Biochim Biophys Acta* **2008**;1780(4):743-9 doi 10.1016/j.bbagen.2008.01.003.

18. Wang L, Zhang J, Wan L, Zhou X, Wang Z, Wei W. Targeting Cdc20 as a novel cancer therapeutic strategy. *Pharmacol Ther* **2015**;151:141-51 doi 10.1016/j.pharmthera.2015.04.002.

19. Sur S, Agrawal DK. Phosphatases and kinases regulating CDC25 activity in the cell cycle: clinical implications of CDC25 overexpression and potential treatment strategies. *Mol Cell Biochem* **2016**;416(1-2):33-46 doi 10.1007/s11010-016-2693-2.

20. El-Deiry WS. p21(WAF1) Mediates Cell-Cycle Inhibition, Relevant to Cancer Suppression and Therapy. *Cancer Res* **2016**;76(18):5189-91 doi 10.1158/0008-5472.CAN-16-2055.

21. Schieke SM, McCoy JP, Jr., Finkel T. Coordination of mitochondrial bioenergetics with G1 phase cell cycle progression. *Cell Cycle* **2008**;7(12):1782-7 doi 10.4161/cc.7.12.6067.

22. Lee HC, Li SH, Lin JC, Wu CC, Yeh DC, Wei YH. Somatic mutations in the D-loop and decrease in the copy number of mitochondrial DNA in human hepatocellular carcinoma. *Mutat Res* **2004**;547(1-2):71-8 doi 10.1016/j.mrfmmm.2003.12.011.

23. Reznik E, Miller ML, Senbabaoglu Y, Riaz N, Sarungbam J, Tickoo SK, *et al.* Mitochondrial DNA copy number variation across human cancers. *Elife* **2016**;5 doi 10.7554/eLife.10769.

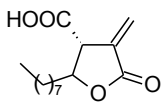
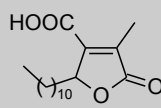
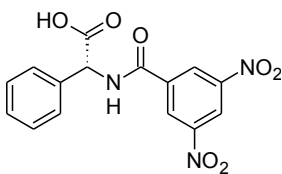
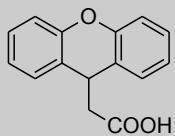
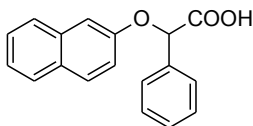
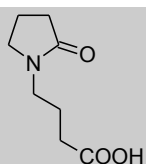
24. Reznik E, Wang Q, La K, Schultz N, Sander C. Mitochondrial respiratory gene expression is suppressed in many cancers. *Elife* **2017**;6 doi 10.7554/eLife.21592.

25. Kuhajda FP, Pizer ES, Li JN, Mani NS, Frehywot GL, Townsend CA. Synthesis and antitumor activity of an inhibitor of fatty acid synthase. *Proc Natl Acad Sci U S A* **2000**;97(7):3450-4 doi 10.1073/pnas.050582897.

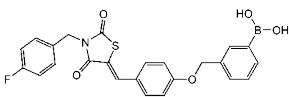
26. Li JN, Gorospe M, Chrest FJ, Kumaravel TS, Evans MK, Han WF, *et al.* Pharmacological inhibition of fatty acid synthase activity produces both cytostatic and cytotoxic effects modulated by p53. *Cancer Res* **2001**;61(4):1493-9.

27. Zhou W, Simpson PJ, McFadden JM, Townsend CA, Medghalchi SM, Vadlamudi A, *et al.* Fatty acid synthase inhibition triggers apoptosis during S phase in human cancer cells. *Cancer Res* **2003**;63(21):7330-7.

Table 1. Chemical library for screening of novel LPA antagonists

| Identification label (trivial name) | Solubility | FW formula | Structure |
|--|----------------|--------------------------------|--|
| C75 | DMSO (EtOH) | 254.32 $C_{14}H_{22}O_4$ |  |
| VS4 (isonephrosterinic acid) | DMSO (EtOH) | 296.40 $C_{17}H_{28}O_4$ |  |
| Q290(dinitrobenzoylPhGly) | DMSO | 345.26 $C_{15}H_{11}N_3O_7$ |  |
| XAA (9-xantenylacetic acid) | DMSO | 240.25 $C_{15}H_{12}O_3$ |  |
| MS25 (b-naphthylmandelic acid) | DMSO | 270.30 $C_{18}H_{14}O_3$ |  |
| OPBA (pyrrolidonylbutyric acid) | DMSO (EtOH) | 171.19 $C_8H_{13}NO_3$ |  |

Commercially available LPAR antagonists

| Identification label (trivial name) | Solubility | FW formula | Structure |
|--|------------|-----------------------------------|--|
| HA130 (HA-130) | DMSO | 463.29 $C_{24}H_{19}BFNO_5S_5$ |  |

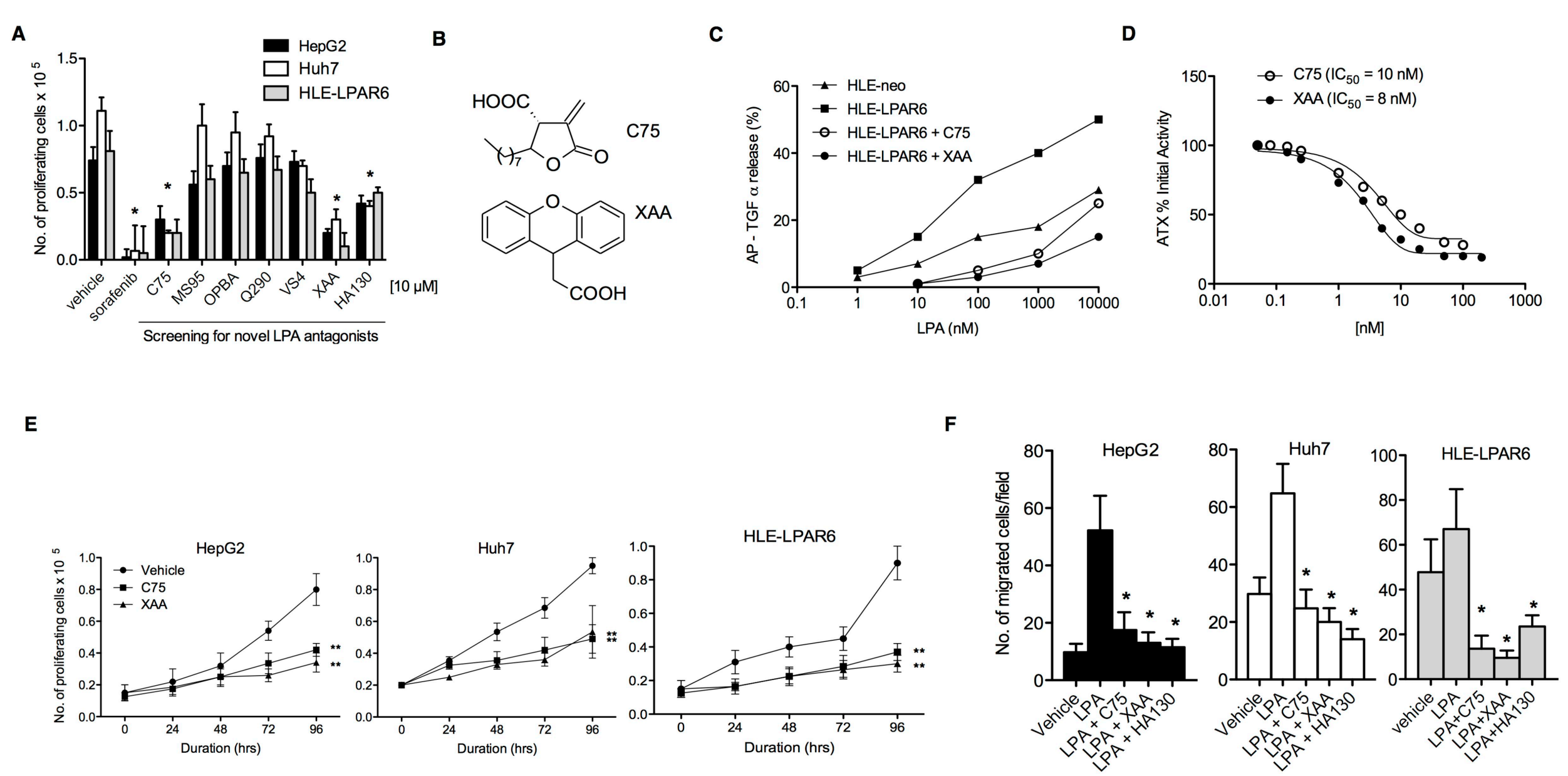
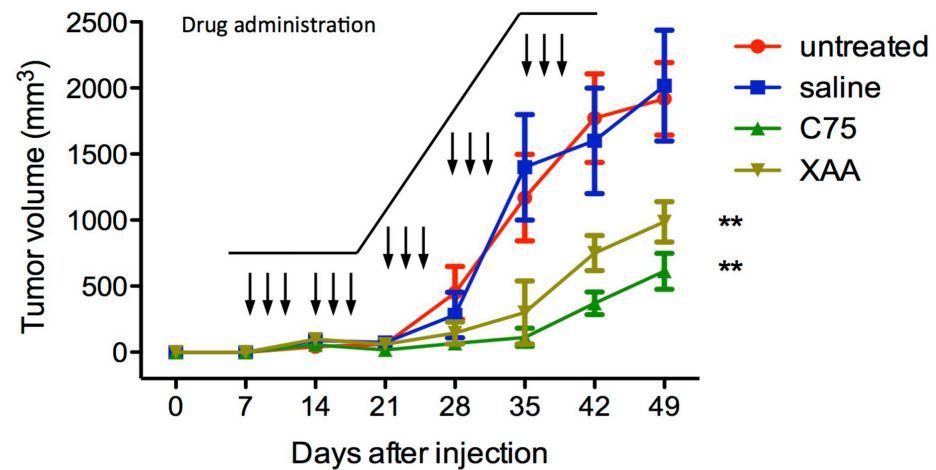
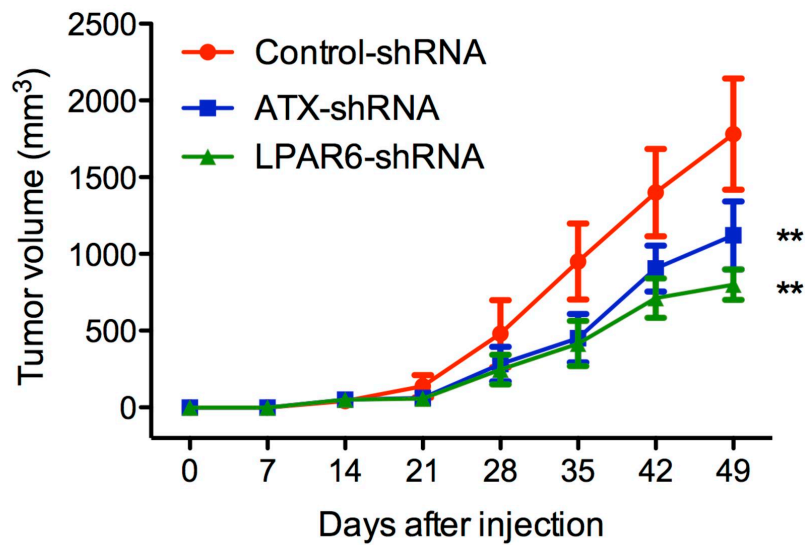
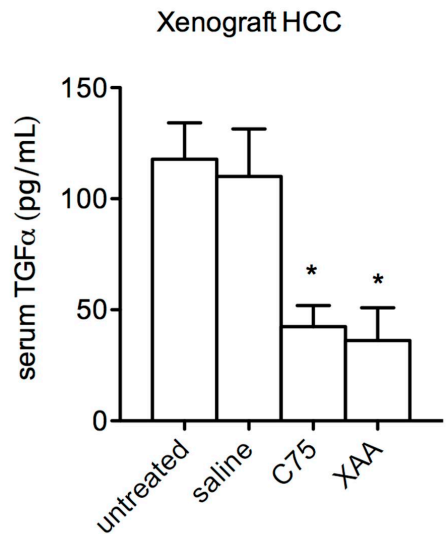
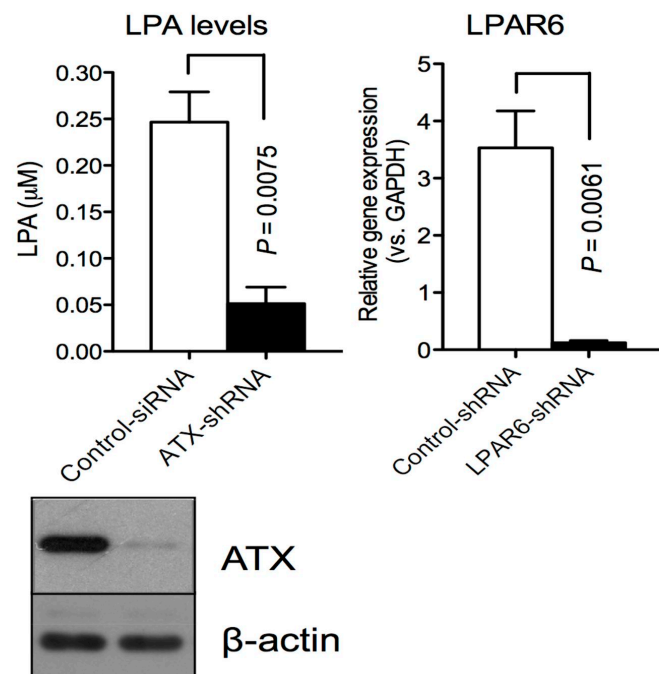
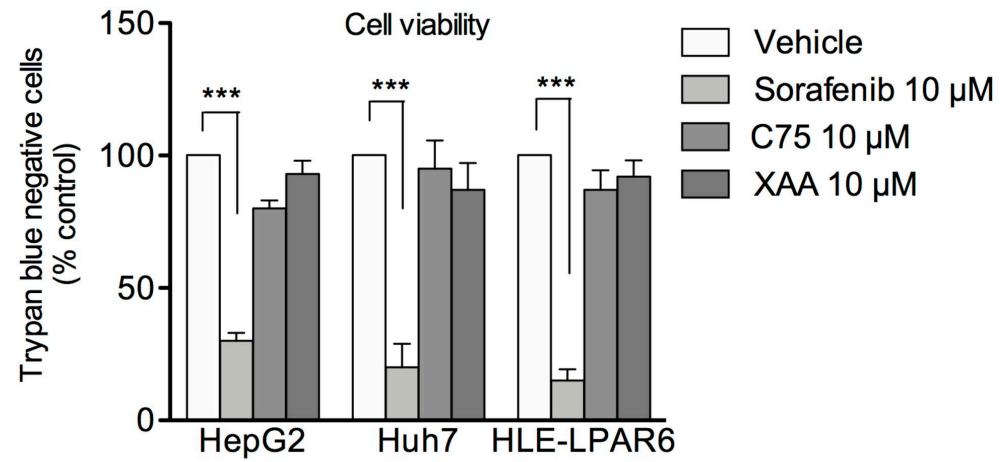
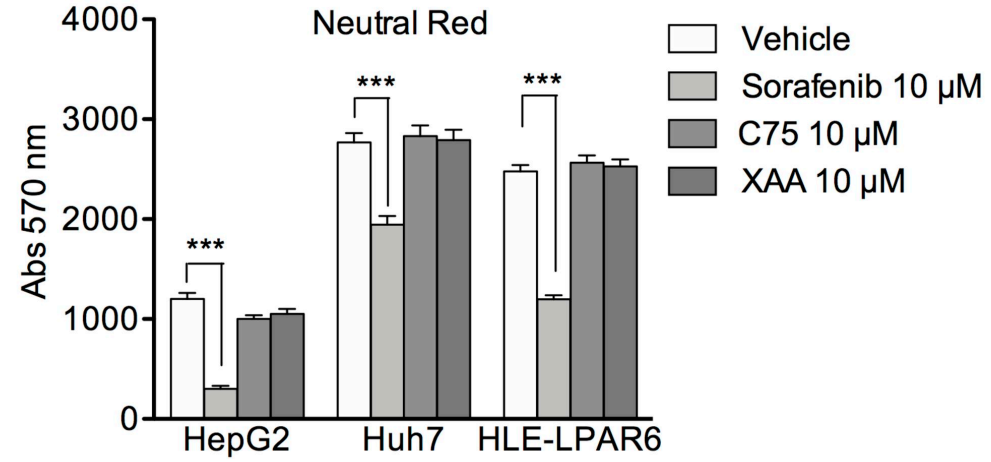
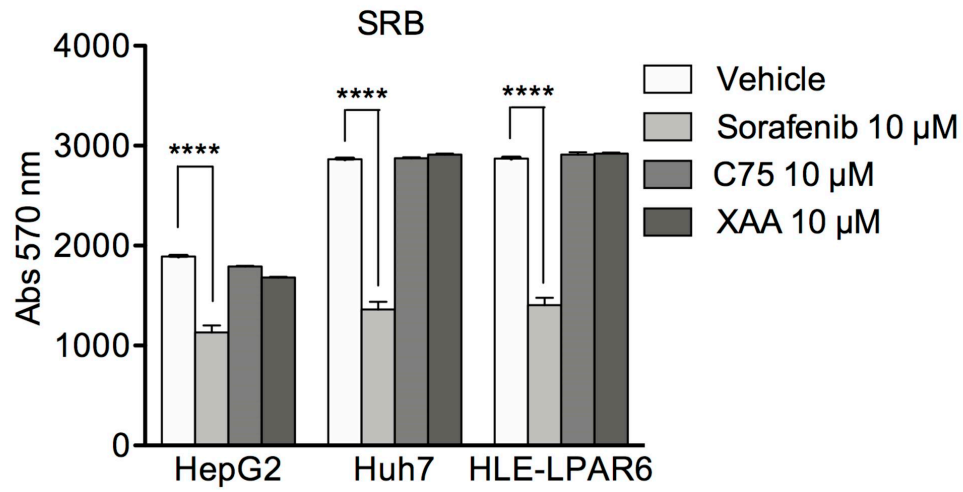
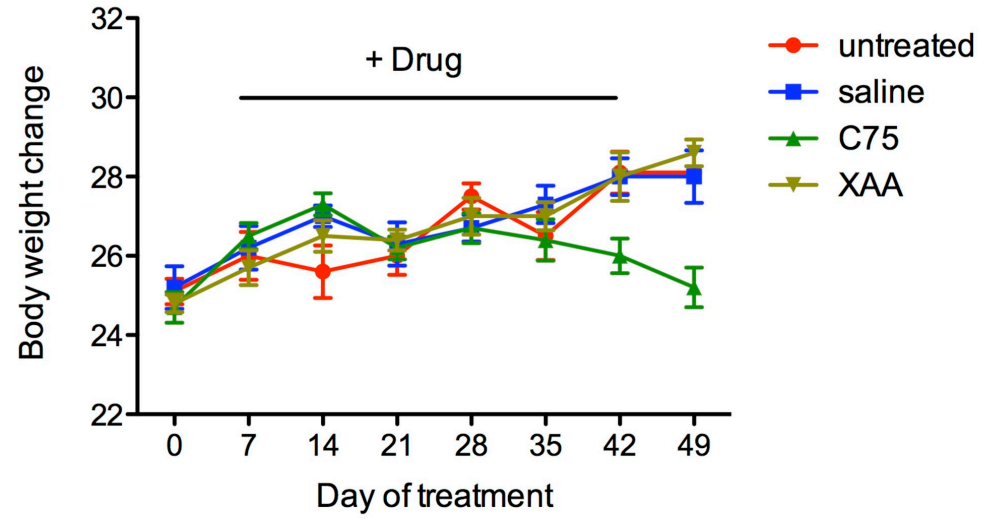


Figure 1

A**B****C****D****Figure 2**

A**B****C****D****Figure 3**

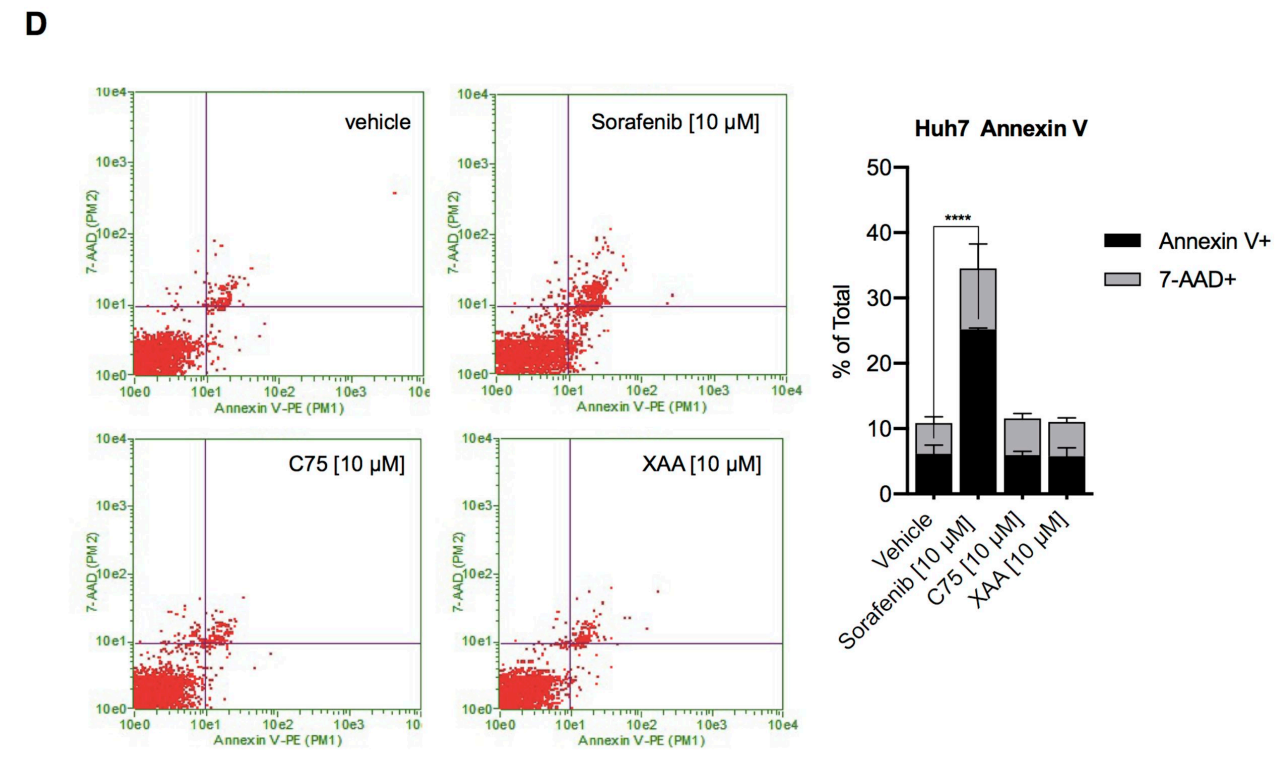
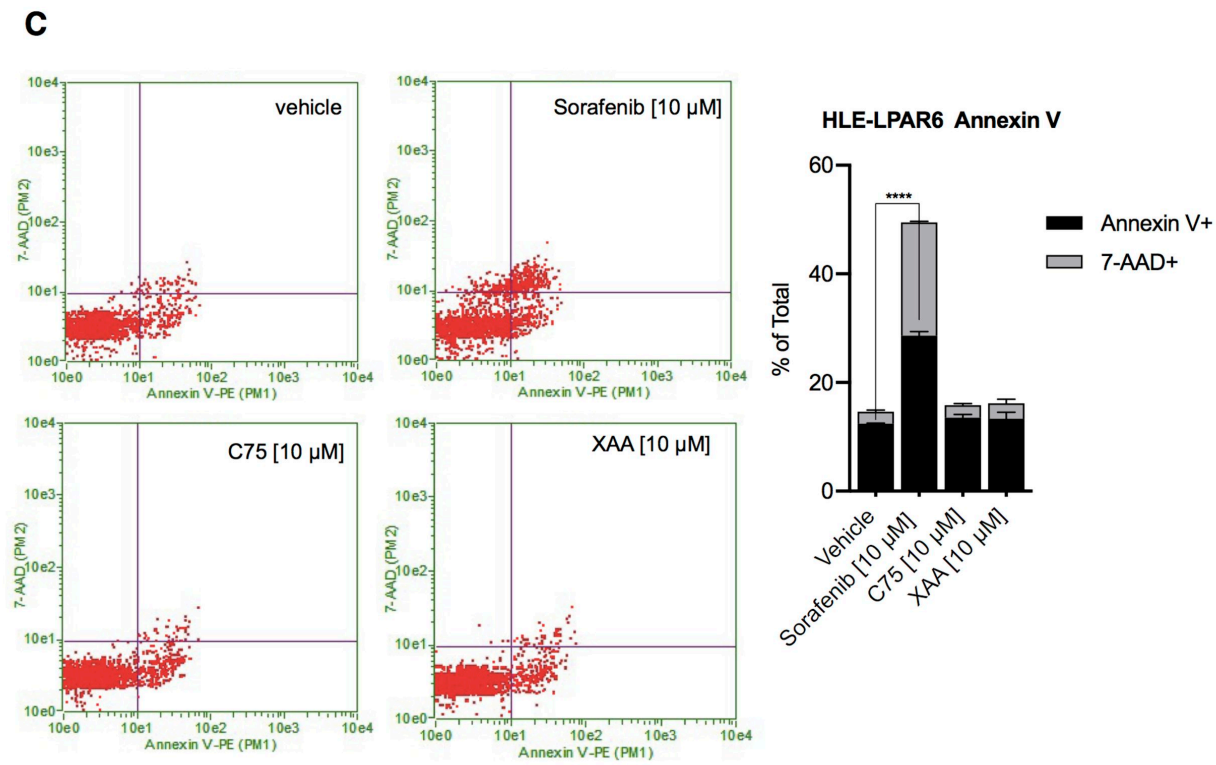
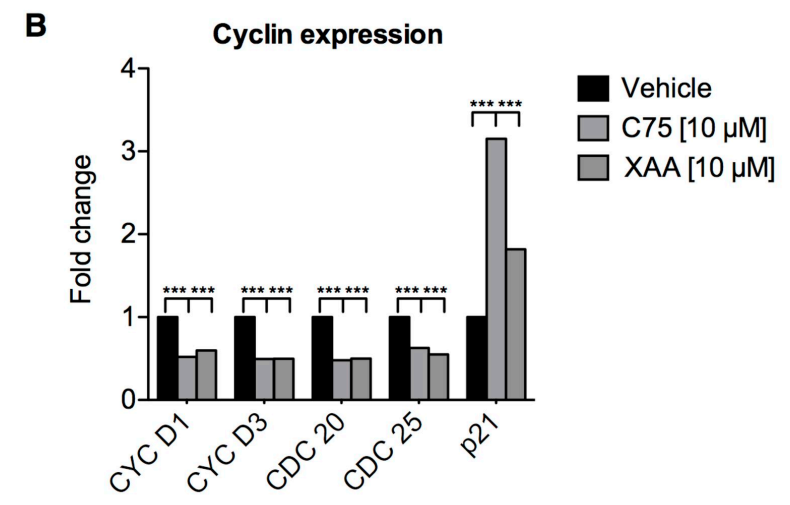
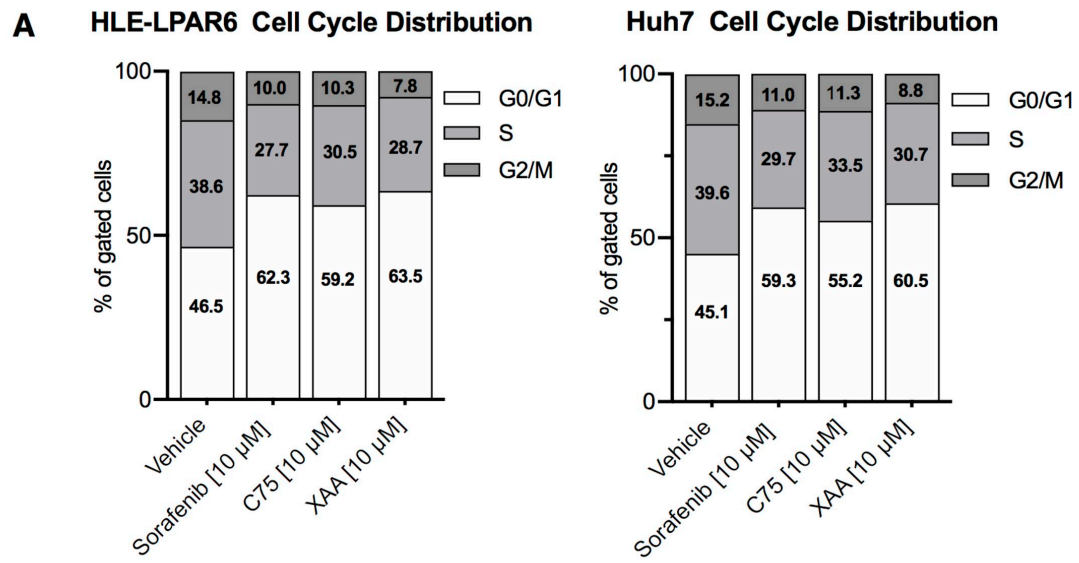


Figure 4

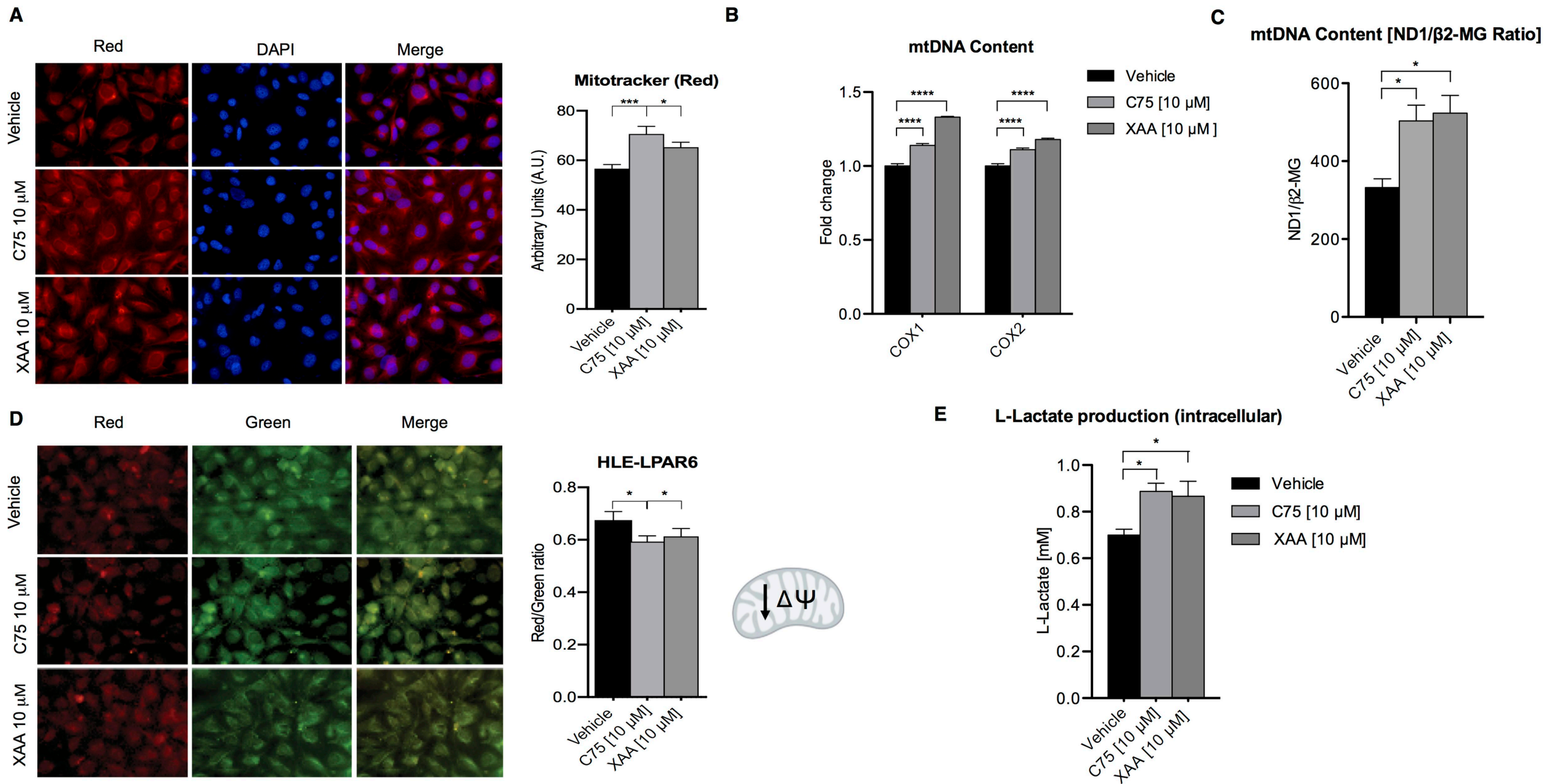


Figure 5